

Full-scale study of conical vortices and roof corner pressures

F. Wu[†], P. P. Sarker[‡] and K. C. Mehta^{††}

Wind Engineering Research Center, Department of Civil Engineering, Texas Tech University,
Lubbock, Texas, 79409-1023, U.S.A.

Abstract. A full-scale synchronized data acquisition system was set up on the roof of the experimental building at the Texas Tech University Wind Engineering Research Field Laboratory to simultaneously collect approaching wind data, conical vortex images, and roof corner suction pressure data. One-second conditional sampling technique has been applied in the data analysis, which makes it possible to separately evaluate the influencing effects of the horizontal wind angle of attack, θ , and the vertical wind angle of attack, ϕ . Results show a clear cause-and-effect relationship between the incident wind, conical vortices, and the induced roof-corner high-suction pressures. The horizontal wind angle of attack, θ , is shown to be the most significant factor in influencing the overall vortex structure and the suction pressures beneath. It is further revealed that the vertical wind angle of attack, ϕ , plays a critical role in generating the instantaneous peak suction pressures near the roof corner.

Key words: conical vortices; full-scale; low-rise building; roof corner; pressure; suction.

1. Introduction

It is generally accepted that high suction pressures occur in the flow separation regions near roof edges and corners of a low-rise building and that the damage of roof cladding is inclined to initiate around these regions. Two typical separated flow phenomena are the separation bubble formed at the leading roof edge by normal winds and the conical vortices generated near the leading roof corner by oblique winds. Various full-scale and wind tunnel model-scale results (Mehta *et al.* 1992, Cochran and Cermak 1992, Ginger and Letchford 1993, Tieleman *et al.* 1994, Lin *et al.* 1995) have shown that the highest suction pressures occur near the roof corner beneath the conical vortices. However, the mechanism for generating these high suction pressures near the roof corners has not been fully understood.

Flow visualization plays an important role in the fundamental research of the pressure-generation mechanism. Clarification of the separated flow phenomenon around the roof corner will result in a better understanding of the pressure-generation mechanism and may improve the wind-tunnel simulation techniques, which can eventually lead to various effective pressure mitigation techniques. Banks *et al.* (2000) performed flow visualization studies on conical vortices in a wind tunnel as part of the Colorado State University (CSU) and Texas Tech University (TTU) Cooperative Program in Wind Engineering (CSU/TTU 1998). Other researchers (Kawai and Nishimura 1996, Kawai 1997, Marwood

[†] Graduate Student

[‡] Associate Professor

^{††} P.W. Horn Professor and Director

and Wood 1997) also applied different techniques to investigate the conical vortex structure in wind tunnels. Full-scale flow visualization was initiated by Wagaman (1993) and Letchford (1995) at TTU to study the separation bubble flow. Thereafter, an extensive study was carried out by Sarkar *et al.* (1997) and Zhao (1997) to visualize the separated flow on the roof of the experimental building at the TTU Wind Engineering Research Field Laboratory (WERFL).

In the past, studies have revealed a direct relationship between the incident wind characteristics, conical vortex structures, and induced pressures. Lateral turbulence of the incident wind is considered to play an important role in this process (Tieleman *et al.* 1996, 1997, Letchford and Marwood 1997).

The goal of the present study is to examine various controlling factors that influence the formation of conical vortices and the subsequent high suction pressures at the roof corners based on full-scale measurements and observations. The experiment supporting this study includes simultaneous visualization of the conical vortices along with measurements of the incident wind data and the roof corner pressures.

2. Experimental setup

The experiment was conducted at the Wind Engineering Research Field Laboratory (WERFL). The WERFL facility consists of a $9.1(\text{B}) \times 13.7(\text{L}) \times 4.0(\text{H})$ m ($30 \times 45 \times 13$ ft) experimental building, a 49 m (160 ft) meteorological tower, and a pressure measuring and data acquisition system which have been fully described by Levitan and Mehta (1992a,b).

2.1. Flow visualization

Visualization of flow patterns can provide us a direct observation and physical understanding of the wind flow fields at different regions around a building. In full-scale experiments, several techniques can be applied to visualize the separated flow phenomena. Sarkar *et al.* (1997) explored a few of these techniques that are suitable for full-scale observation. These include tuft-grid, airfoil-grid, and smoke-injection methods. In this study of the conical vortex case, the tuft-grid method was employed for its fast response to the highly turbulent conical vortex flow and effectiveness to capture the instantaneous characteristics of the conical vortices. The yarn strands used as tufts in this method are so soft and light that they can move and align with the flow streamlines and fluctuate instantaneously corresponding to the turbulence of the flow within the relatively small dimension of a conical vortex.

A 2.13 m (7 ft) long by 1.02 m (3.33 ft) high tuft-grid frame with a mesh size of 10.2 cm (4 in) square was built for this experiment. A bright white yarn strand with a length of 17.8 cm (7 in) was tied at each node of the thin steel wire mesh. The grid was placed at different locations close to a roof corner—normal to the corner diagonal bisector line in one case and perpendicular to the short roof edge in another case—to visualize either a pair of conical vortex or only one conical vortex on the plane of the grid, respectively. The results presented in this paper pertain to the grid placed perpendicular to the short roof edge. Flow visualization experiments were carried out at night to obtain better visualization of the vortices without any interference from background lights. Two floodlights were used to illuminate the tuft-grid.

2.2. Synchronized data acquisition system

To study the conical vortex flow phenomenon, the vortex images need to be simultaneously

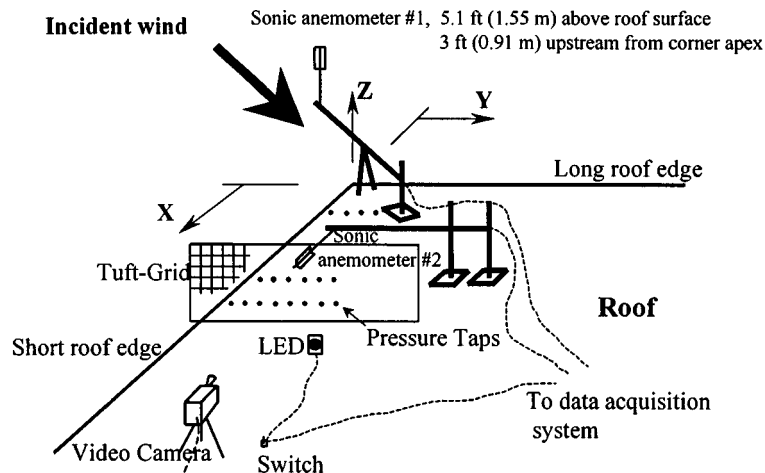


Fig. 1 Synchronized data acquisition system

recorded and synchronized with both incident cornering wind data and corner pressures. Fig. 1 schematically illustrates the experimental setup of the synchronized video, wind, and pressure data acquisition system. Vortex images were recorded by an 8-mm video camera at a speed of 30 frames/second. An LED (Light Emission Diode) was placed between the video camera and the tuft-grid to provide a source of light to the camera along with a voltage signal to the data acquisition system. The vortex images and light signals were recorded by the camera; while the wind and pressure data together with the LED voltage signals were collected by the data acquisition system at a frequency of 30 Hz. Thus, the LED virtually acted as a synchronizer in simultaneously relating the vortex images with the wind and pressure data. Through viewing and identifying the light signals in the video and the LED voltage jumps stored in the collected data run, video images and other data can be fully synchronized. Unfortunately, this manual process is a very time-consuming and painstaking step in the whole data processing and analyzing procedure. Two sonic anemometers were selected to measure the wind flow velocity for their sufficiently high frequency response. Sonic #1 was installed on the tip of a supporting stand overhanging upstream bisectionally from the roof corner apex to measure the upstream incident wind velocity (location specified in Fig. 1). Only for several limited runs, Sonic #2 was placed at different points above the roof surface to measure the flow velocity within the conical vortices.

The reasons for the particular location of Sonic #1 are to minimize the influence of the building on the incident wind and to capture the closest and reliable upstream wind data for better correlation with the video images and pressures. Since acquiring reliable incident wind data is important to this experiment, another independent experiment was conducted to study the wind characteristics at this point (Wu 2000). By comparing sonic anemometer measurements of wind velocities at the roof corner and at 4 m (13 ft) height on the meteorological tower, it has been proven that the wind measured at the specific location above the roof corner can represent freestream wind quite accurately after correcting for the difference in height between the two sonic anemometers. For the wind measurements at the specific point near the roof corner, the longitudinal and lateral components of wind velocity remained unchanged; the fluctuating part of the vertical component was found to be consistent with freestream wind at the same height. Unlike the freestream wind, the vertical

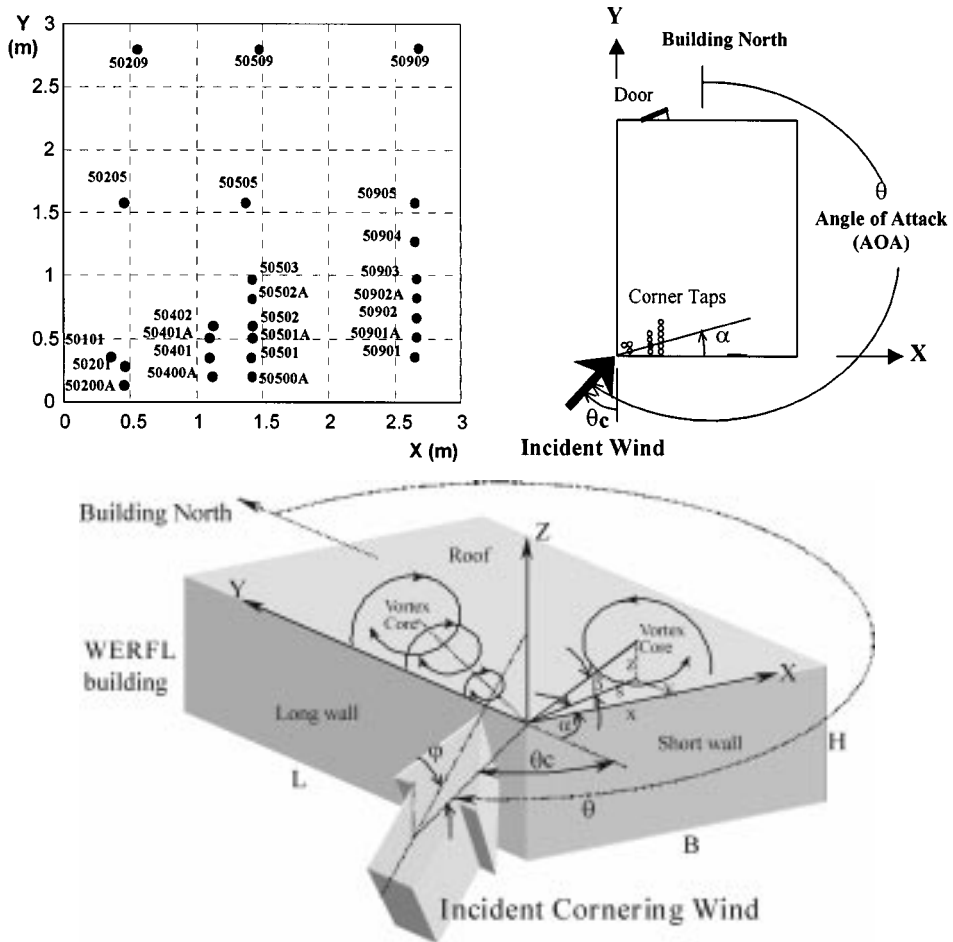


Fig. 2 Corner pressure tap locations and definition of coordinates and angles for WERFL experimental building

component of the wind velocity near the roof corner held a small positive mean value, as expected.

2.3. Pressure tap arrangement and nomenclature

The corner pressure taps were densely arranged close to the short roof edge. Fig. 2 shows the layout of all pressure taps near the WERFL roof corner and defines the coordinates and angles needed to clearly describe the incident wind direction and conical vortex position and structure. Note the dense array of pressure taps compared to what is described by Levitan and Mehta (1992a,b) and angle ϕ employed to define the vertical wind angle of attack (or pitch angle).

3. Results and discussion

Systematic experiments and measurements were conducted at the WERFL experimental building. Over 100 data runs, each of 15-minute duration, were collected, which also include cornering

incident wind information. Out of these data runs, fifty-five runs were validated through WERFL standard data validation procedure.

3.1. Conditional sampling technique

The natural wind is a highly turbulent flow phenomenon. Even in a relatively short 15-minute period, the incident wind changes its speed and direction frequently and abruptly (Zhao 1997, Wu 2000). Large fluctuations for the horizontal wind angle, θ , in an order of 30° per 1/30 second and within a range of 100° , and for the vertical wind angle, φ , in an order of 20° per 1/30 second and within a range of 70° were observed in a 15-minute period. These highly turbulent characteristics of the natural wind cause unsteadiness of the conical vortex flow and make it extremely difficult to detect the linkage between the incident wind and the conical vortices. Hence, the conventional 15-minute run-average data are less informative for analyzing the conical vortex flow.

A conditional sampling technique has been employed to solve this problem. The basic idea is to sample very short consecutive data segments, which satisfy some prescribed conditions, from the typical 15-minute data runs. In the beginning, a 3-second period was used to analyze the relationship between the horizontal wind angle of attack and the vortex structure (Wu *et al.* 1999). During the process of data analysis, it was further realized that the vertical wind angle of attack might also play a substantial role in the conical vortex flow phenomenon and needs to be considered. Subsequently, a 1-second time period was applied. In the process of extensive data sorting and sampling, it was observed that the overall vortex position and structure sustain very well within this 1-second short period and that the instantaneous wind speed fluctuations have negligible influence on the overall vortex position and structure. To better study the relationship between the conical vortex and the underlying pressures, the influence of the wind speed variation was isolated from the pressure coefficients by normalizing the surface pressures with instantaneous wind dynamic pressure measured at the roof corner. This treatment resulted in the so-called *instantaneous pressure coefficients* that will be used in the following analysis.

Briefly, the 1-second conditional sampling method is to extract all possible 1 second long, consecutive time series from the typical 15-minute data run for both wind, pressure data, and the synchronized vortex images. The sampling process is triggered whenever the following conditions are satisfied :

- (a) Horizontal incident wind angle of attack (AOA), θ , fluctuates no more than $\pm 5^\circ$ about the 1-second mean horizontal AOA in that 1-second period; and
- (b) Vertical incident wind AOA, φ , fluctuates no more than $\pm 4^\circ$ about the 1-second mean vertical AOA in that 1-second period.

Around 420 image-synchronized 1-second data segments were sorted out in this study. The 1-second mean values of wind and pressure data and the corresponding 1-second averaged parameters (α_c —vortex core angle, α_r —vortex reattachment point angle, and β —vortex core vertical angle as illustrated in Fig. 2) describing the vortex position and structure are then calculated for each 1-second data segment for further analysis. The limitations of wind angle fluctuations could be prescribed more strictly, but this only results in scarcity of sorted data and makes subsequent analysis difficult.

3.2. Conical vortex structures and controlling factors

Vortex images used in this paper correspond to four different planes perpendicular to the short

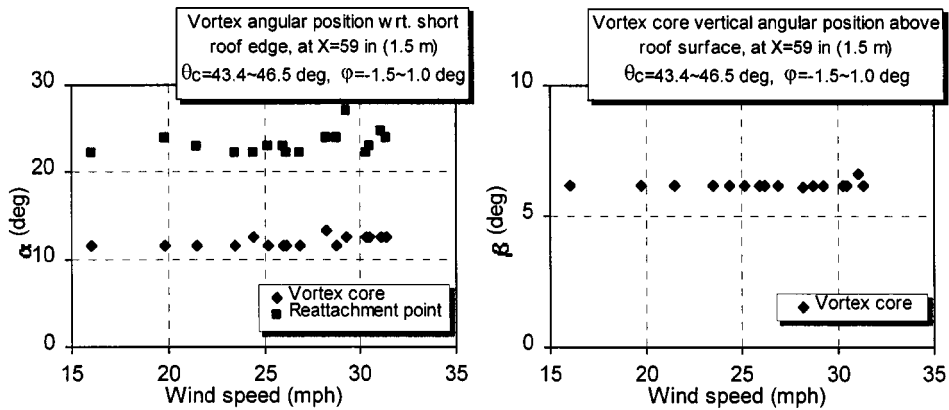


Fig. 3 Influence of incident wind speed on conical vortex structures

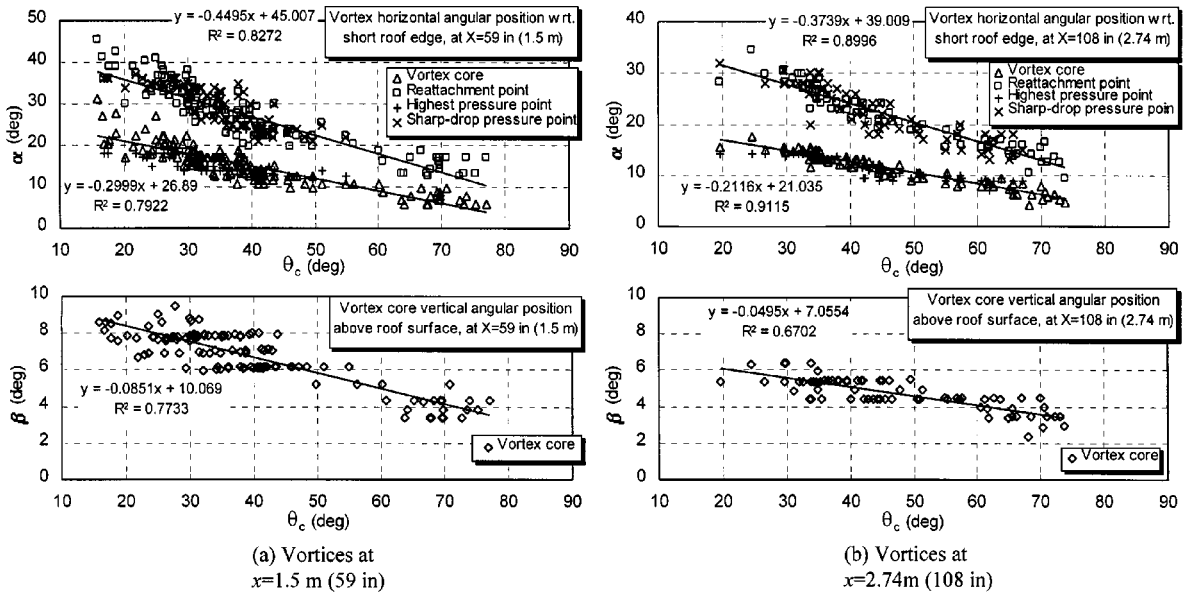


Fig. 4 Influence of horizontal wind angle of attack on conical vortex structures

roof edge and close to the roof corner apex at $x=1.19$ m (3.92 ft), 1.5 m (4.92 ft), 2.06 m (6.75 ft), and 2.74 m (9.0 ft), respectively.

Fig. 3 illustrates the influence of incident wind speed on the conical vortex parameters describing its position and structure for the case when θ_c ($\theta_c=\theta-180^\circ$) and φ are approximately constant. It is clear that the wind speed has no obvious effect on the position and structure of the vortex. This generally implies that the wind speed fluctuations only affect the strength of the vortex but not the overall structure. It also justifies the use of instantaneous pressure coefficient to remove the direct effect of wind speed on the conventional pressure coefficient.

Fig. 4 demonstrates the influence of the horizontal wind angle of attack, θ_c , on the overall vortex structure. No attempt was directed to separate the effect of the vertical wind angle of attack, φ , from

the data set shown in this figure. Fig. 4 clearly reveals the dominant effect of θ_c on the position and structure of the conical vortex. The conical vortex parameters (α_c , α_r , and β) vary linearly with θ_c . Although a quadratic curve may fit some of the data group better, linear regression is still applied to the entire data group for simplicity. Regression lines and equations are listed in Fig. 4. The large R^2 values (coefficient of determination) listed beside the regression lines clearly exhibit an approximate linear relationship between θ_c and the conical vortex parameters. The size of the conical vortex near one roof edge increases linearly with the horizontal wind direction, as the wind gets more and more perpendicular to that roof edge. For all vortices observed at different locations in this experiment, the inclined angle of reattachment point α_r is generally double of the inclined angle α_c of the vortex core. This feature of the conical vortex structure can help to improve our understanding of the overall vortex structure and the underneath pressure distribution. The favoring angle of attack, θ_c , for conical vortex formation can also be confirmed falling in the range of $15^\circ \sim 75^\circ$, which agrees with the observation by Lin *et al.* (1995).

The results shown in Fig. 4 have been compared to the results of wind tunnel experiments (Marwood and Wood 1997, Banks *et al.* 2000). The wind tunnel results roughly match our full-scale results, but differences do exist (Wu 2000).

The conical vortex core traces that were projected on the WERFL roof surface are presented in Fig. 5 for several selected angles θ_c . Second-order polynomial regression fits the data quite well. In this figure, the conical vortex core trace on the roof surface is not extending along a straight line from the roof corner apex; rather, it is slightly curving toward the roof edge. This characteristic of vortex core trace needs to be considered when we describe the conical vortex core location projected on the roof by using the ray angle extending from the roof corner apex.

Several typical conical vortex images at two different locations are shown in Fig. 6 to provide a direct perception of different vortex structures. These vortex images are observed for very small φ . Thus the obvious difference of the conical vortex structure at any location is mainly caused by θ_c .

Although not as significant as θ_c , the vertical wind angle of attack, φ , also substantially influences

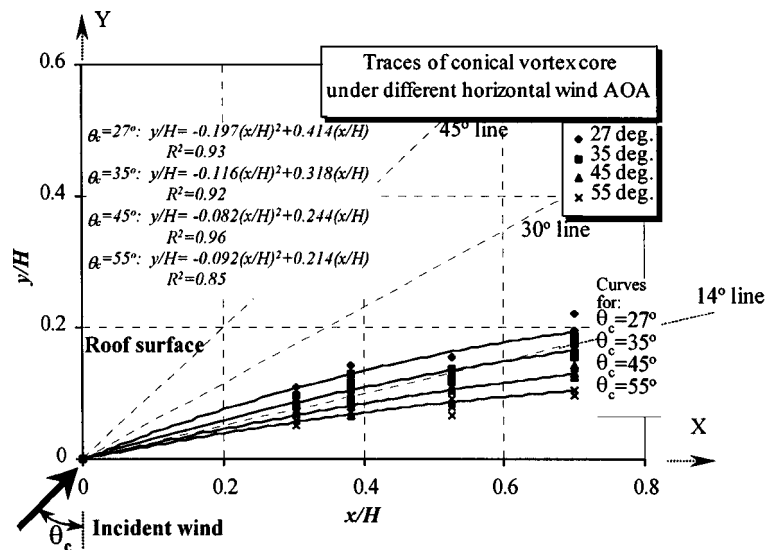


Fig. 5 Conical vortex core traces projected on roof surface near the corner.

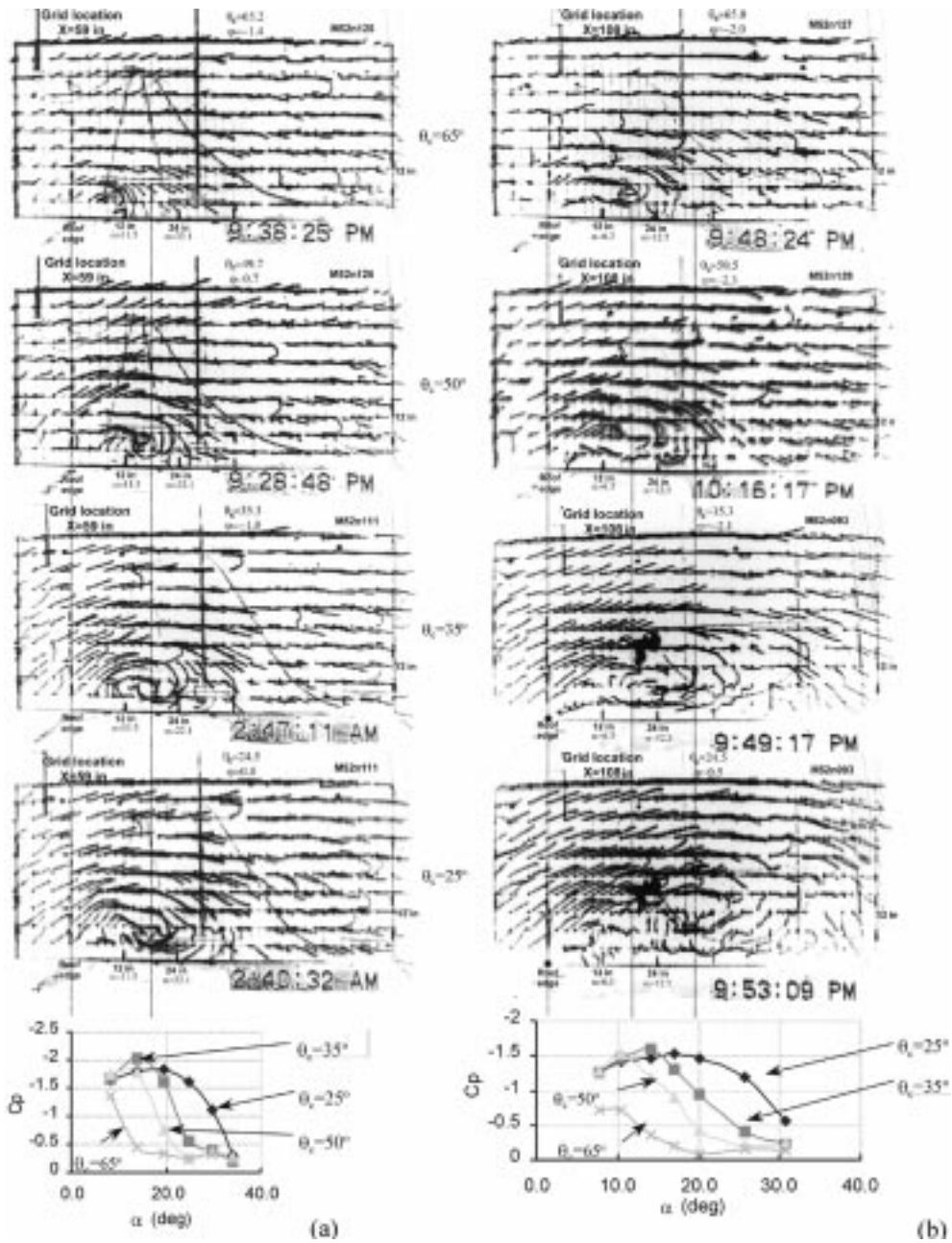


Fig. 6 Conical vortex images for different horizontal angles of attack θ_c . (a) At $x=1.5$ m (59 in), (b) At $x=2.74$ m (108 in)

the overall vortex structure. Fig. 7 displays the relationship between φ and the vortex parameters for nearly constant θ_c . The data reveal that the size of the conical vortex generally increases with increasing (more positive or upward) φ . Observation of the influence of φ on the overall vortex structure for different angles θ_c shows that influence from φ is stronger for small vortices when θ_c is large (close

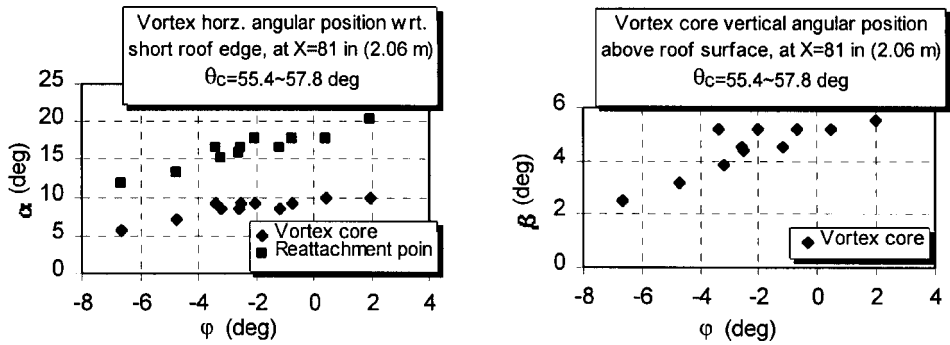


Fig. 7 Influence of vertical wind angle of attack on conical vortex structures

to 90°). However, compared to the dominant effect of θ_c , the effect of ϕ is only secondary. It is important to notice that, under the limitation of 1-second sampling conditions, data segments for large values of ϕ are sparse. Thus, the above conclusion is only induced from limited variations of ϕ . It is possible that for very large variations (over 20°), ϕ can also remarkably influence the conical vortices and pressures.

Vortex images to illustrate the influencing effect and extent of ϕ on the overall vortex structure are exhibited in Fig. 8. The images clearly show the higher and longer separated shear layers and larger vortices induced by larger ϕ .

3.3. Conical vortex induced suction pressures

In Figs. 6 and 8, one-second mean pressure profiles underneath different vortices are shown with the same length scale of the corresponding vortices to facilitate comparison between them. For all cases shown in these figures, the direct relationship between the vortex and its induced pressures underneath is obvious and consistent. The peak suction point of pressure profile basically corresponds to the vortex core position; while the suction drops sharply to a very small value in the region close to and beyond the vortex reattachment point.

If we define the peak suction point and the point right after the sharp drop in suction on the pressure profile as *highest pressure point* and *sharp-drop pressure point* respectively, we can directly compare them with the vortex structure parameters α_c and α_r . The *highest pressure points* and *sharp-drop pressure points* have already been included in Fig. 4. It is apparent that the *highest pressure point* coincides with the vortex core position and the *sharp-drop pressure point* coincides with the flow reattachment point for nearly all angles θ_c shown in the figure.

It can also be concluded from the pressure profiles in Figs. 6 and 8 that high suction pressures generally occur in a wedge-like region on the roof corner surface bounded by the 30° ray extending from the roof corner apex and the referred roof edge. This region can be referred as the vortex-prone region. Another feature that is revealed by the pressure profiles in Figs. 6 and 8 is that for each line of pressure taps, the highest pressure points of the pressure profiles do not differ much and are relatively close to each other for a wide range of θ_c between 25° and 50° . It can be tentatively assumed that high suction pressures may be generated through a wide range of horizontal angles of attack at points close to the 14° ray line.

Since high suction pressures basically follow the trace of vortex core, the surface suction pressure

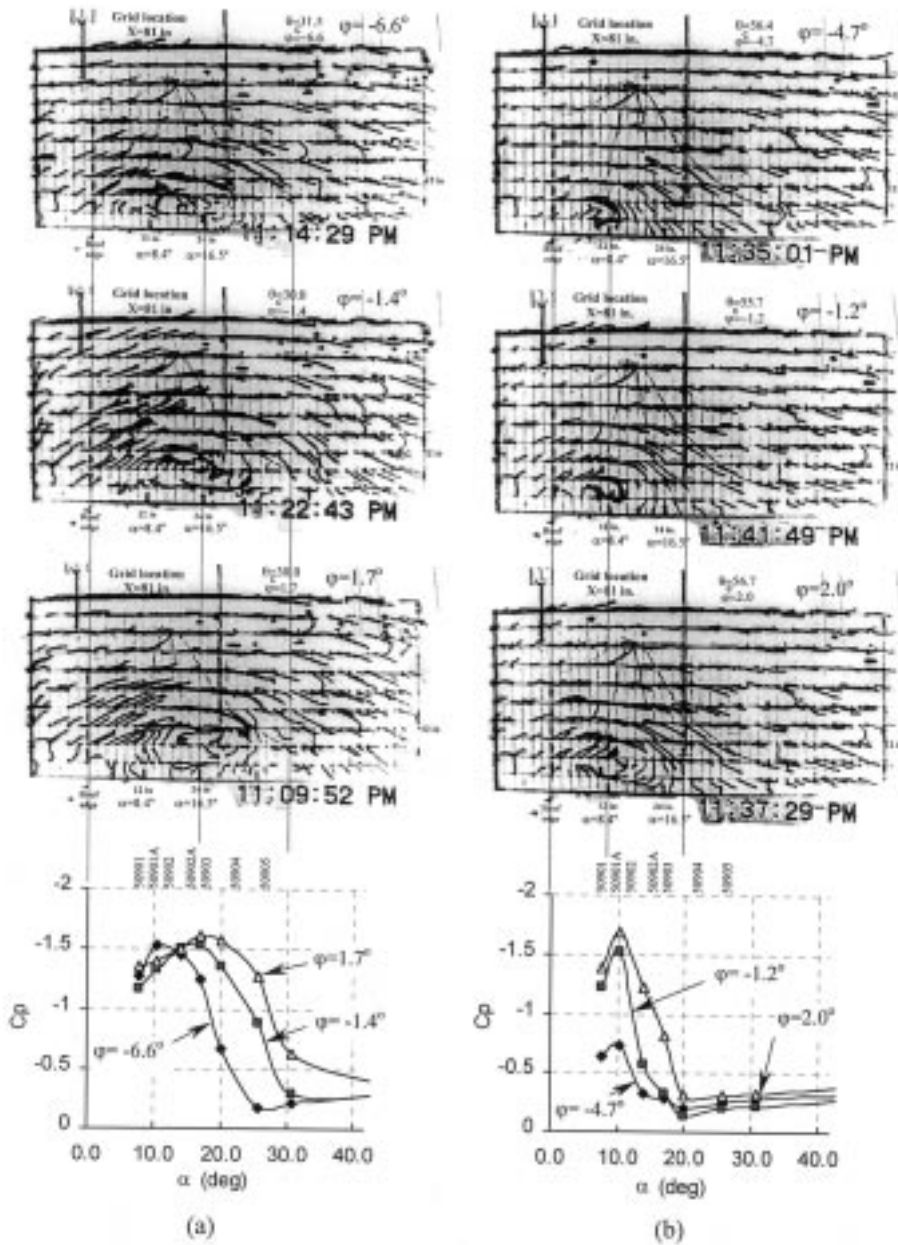


Fig. 8 Conical vortex images for different vertical angles of attack ϕ . (a) Horizontal angle of attack $\theta_c=30^\circ$, (b) Horizontal angle of attack $\theta_c=56^\circ$

at any point near the corner will reach its highest value whenever the incident wind takes the favoring angles θ_c and ϕ to generate a vortex right above that point.

Fig. 9 compares the effects of horizontal and vertical angles θ_c and ϕ on the pressures. It can be concluded that θ_c primarily dominates the pressure distribution; while ϕ only gently expands or contracts the size of the vortex and thus modifies the pressure distribution profile to a relatively

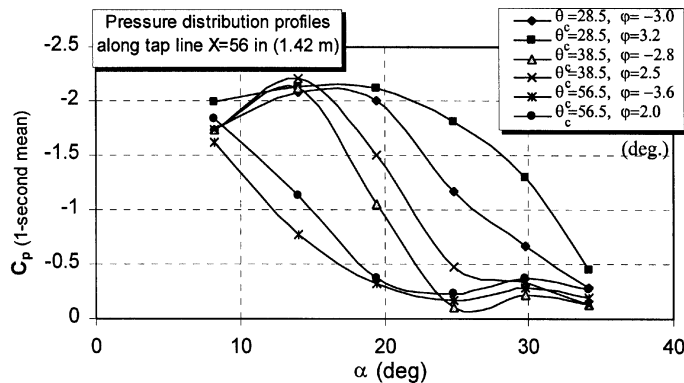


Fig. 9 Influence of horizontal and vertical wind angles of attack θ_c and φ on pressure coefficients near roof corner

small extent. However, it is important to point out that the influence of φ is large and obvious for the point pressures close to the reattachment point of the vortex. Since φ can affect the size of the vortex, for the points near the vortex reattachment point, the points previously not covered by the vortex may be covered after an increasing φ has expanded the size of the vortex, and this will result in a substantial increase of suction at that point.

3.4. Generation of instantaneous peak suction pressures

Extreme value cross-correlation analysis reveals that large fluctuations of suction pressure are highly correlated with the large fluctuations of the vertical component of incident wind in the vortex-prone region, especially in the vortex flow-reattaching region. This further confirms the influence of φ on vortex structure and the induced pressures beneath.

Tieleman *et al.* (1996) revealed the increase in magnitude of the peak suction pressure coefficients with increasing lateral turbulence intensity. Zhao (1997) also indicated the importance of the horizontal wind direction fluctuations in generating peak suction pressures. While similar effect of the fluctuations of the horizontal wind angle of attack in inducing the peak suction pressures was also observed in this study, it was further noticed that the vertical wind angle of attack might play an even more important role in the generation of instantaneous peak suction pressures.

Due to the limitation of this paper's length, it is not our primary intention to extensively discuss the instantaneous peak suction pressures. A detailed discussion can be found in Wu (2000). Only one of the many interesting segments of data time history is picked out and presented here in Fig. 10 to display the role of the vertical wind angle, φ , in generating the instantaneous peak suction pressures. The figure clearly reveals the inherent link between large positive excursion of φ and peak suction pressures. Instantaneous peak suction pressures are clearly associated with large and fast upward fluctuations of φ . Whenever a large fluctuation of φ occurs, the role of the horizontal wind angle, θ , in affecting the vortex structure and the pressures becomes less important while θ falls in the favoring range for generating an initial (or prototype) vortex. Synchronized vortex images confirmed that large upward excursion of φ raised the height of separated shear layers and increased the size and height of the conical vortex significantly.

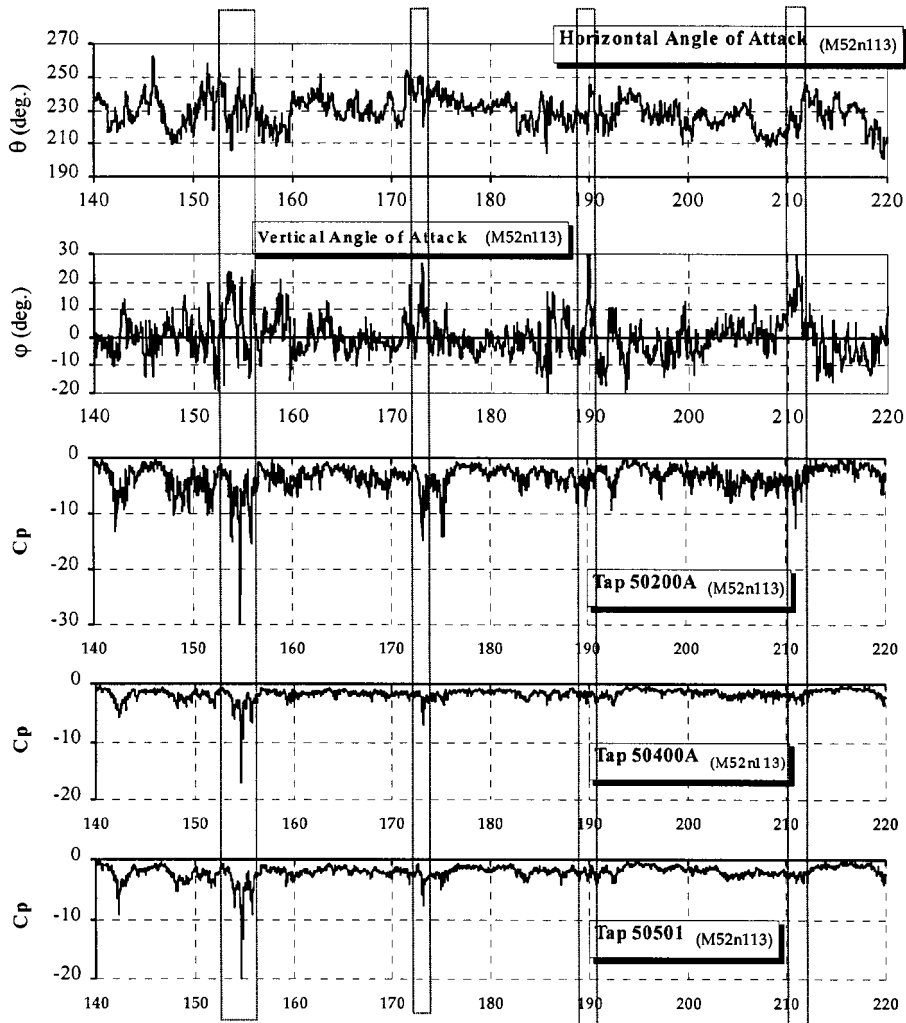


Fig. 10 Generation of instantaneous peak pressures (C_p -instantaneous pressure coefficient)

3.5. Features of the conical vortex flow

Spectral analysis of the fluctuating pressures shows a local peak of energy content near the frequency $n \approx 5$ Hz for point pressures in the vortex-prone region. This highly turbulent content can be attributed to the intermittent nature of the conical vortex, which is commonly called the *building generated turbulence*.

Compared to the transient nature of the separation bubble flow formed on the roof by normal winds, the conical vortex flow is a relatively continuous and steady separated flow phenomenon. As long as the cornering incident wind has sufficient energy (when the wind speed exceeds 5 m/s approximately), conical vortices will be formed which will keep resizing and swaying according to the change of wind angle of attack. While the conical vortex flow looks like a continuous flow for a normal speed observation, a close scrutiny of the flow process reveals its intermittent characteristic,

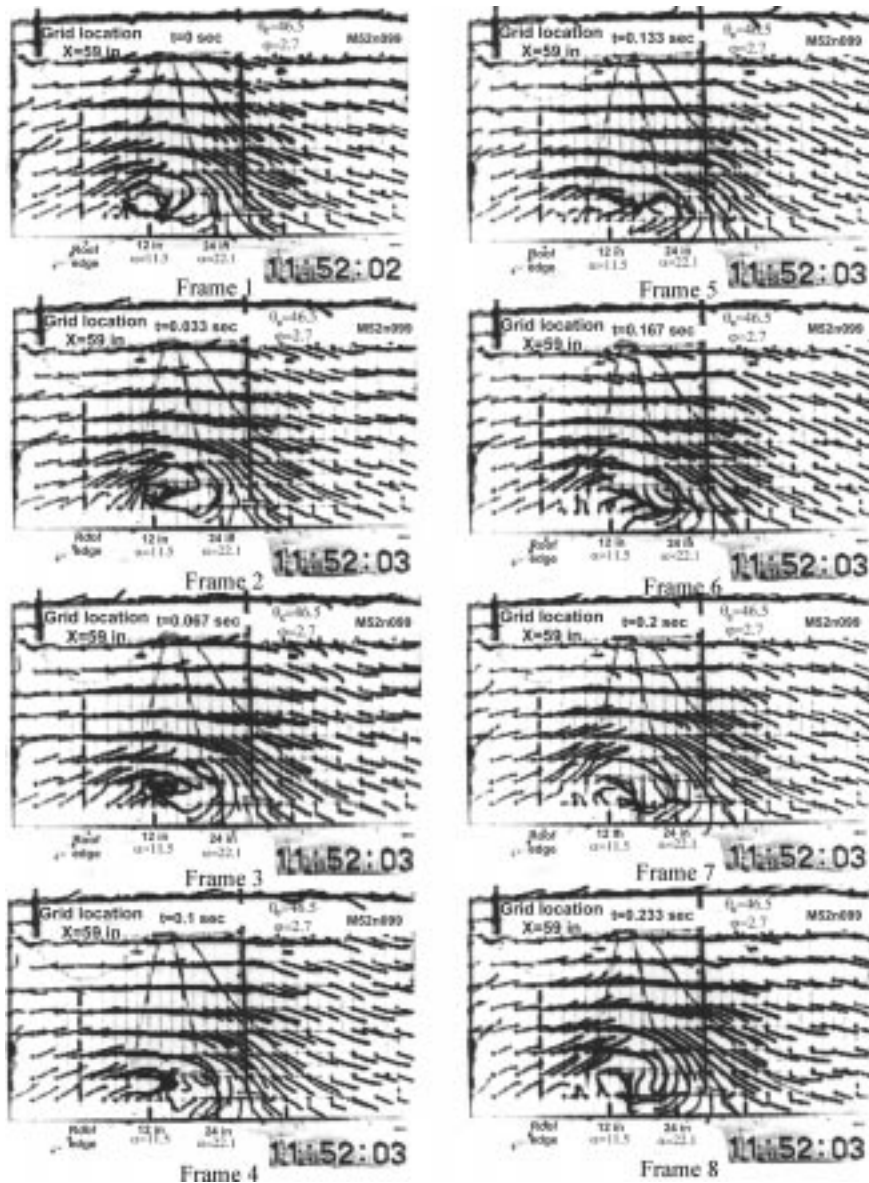


Fig. 11 One cycle of conical vortex formation and development (time interval between consecutive frames—1/30 second)

which is the cause of very high frequency fluctuations of the corner pressures.

Fig. 11 illustrates the whole process of the conical vortex formation through a sequence of consecutive vortex images. The time interval between images is 1/30 second. Incident wind speed at the moment is around 6.3 m/s (14 mph). The conical vortex is basically sealed in a bubble-like field bounded by the separated shear layers starting from the sharp roof edge and ending at the reattachment point. At the moment when the conical vortex is formed (frame 1 in Fig. 11), it rolls up (tightens up) toward a higher and closer position with respect to the roof edge and grows up to a full strength (frames 2

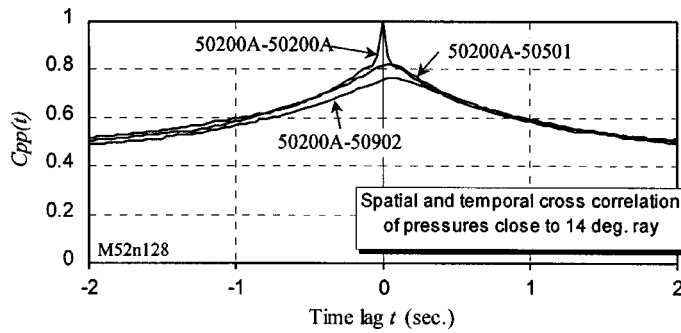


Fig. 12 Spatial and temporal cross-correlation between three tap pressures along the conical vortex core traces (Reference pressure tap-50200A)

and 3). Then it is convected a very short distance downstream (frame 4). In the meantime, when it is moving away from the roof edge, the vortex loses the necessary driving force and starts to dissipate. It becomes more flattened and so is the curvature of the separated shear layers (frames 4 and 5). This process leads into the collapse of the vortex structure (frame 6). But at almost the same instant, it re-grows and tightens up again (frames 7 and 8). Then the entire process repeats itself. This entire process occurs in a very short period of time, approximately 0.25 second, i.e., at a characteristic frequency of 4 Hz. This characteristic frequency of conical vortex intermittency seems to change proportionally with the incident wind speed, which helps to explain the local high energy content of pressure fluctuations at frequency $n \approx 5$ Hz, since the pressure fluctuations in this range of high frequency are obviously not induced by incident wind turbulence (lack of energy in this range).

Spatial and temporal cross-correlation between the roof corner pressures at different locations has also been investigated. Fig. 12 shows the pressure cross-correlation between taps along the conical vortex core traces as illustrated in Fig. 5. It is evident that the fluctuating pressures underneath the conical vortices are highly correlated and the time delay for the highest correlation point of each curve is negligible, considering the long distance between those taps. This means that high suction pressures along the roof edge occur almost simultaneously. A similar result was also given by Letchford (1995). The high pressure correlation and negligible time delay imply that the vortices along the roof edge are coherent and the strip-like-area-averaged pressures near the roof edges

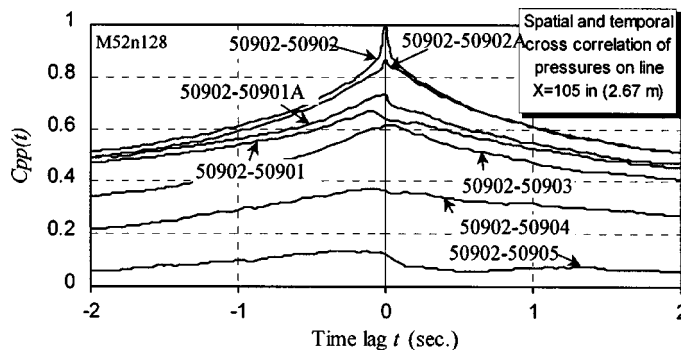


Fig. 13 Spatial and temporal cross-correlation between tap pressures along a line perpendicular to short roof edge (Reference pressure tap-50902)

should be higher than those averaged over other areas.

Pressure cross-correlation between taps along the line of $x=2.67$ m (8.75 ft) is given in Fig. 13. High correlation of pressure fluctuations exists between tap 50902 and taps from 50901 up to 50903. These taps are located in the vortex-prone region. Fluctuating pressures for taps beyond 50904 are less of correlation with those of 50902, as these taps are close to or totally out of the vortex-reattaching region. The total time delay from tap 50901 to tap 50903 is small but still discernable to be a period of 0.13 second. This small period may be inherently caused by the intermittent characteristic of the vortex mentioned above.

4. Conclusions

Through analyzing the synchronized data set of the incident wind, vortex images, and corner pressures collected at the Texas Tech Wind Engineering Research Field Laboratory experimental building, the direct relationship between the incident wind, conical vortices, and the associated high suction pressures has been further clarified.

It is found that the high suction pressures near the roof corner are generated directly underneath the conical vortex core position and drop off sharply to very low magnitudes near the vortex reattachment point. Main characteristics of the incident wind that influence the position and structure of the conical vortex, in the order of significance, are the horizontal wind angle of attack, θ , and the vertical wind angle of attack, φ . The main characteristics of the incident wind that influence high suction pressures underneath the conical vortex can then be summarized as the incident wind speed, the horizontal wind angle of attack, θ , and the vertical wind angle of attack, φ . These three factors may contribute in different proportions to the generation of pressure at different locations on the roof.

Another major finding is that the vertical wind angle of attack, φ , plays a very critical role in the instantaneous peak suction pressure generation. Thus, besides the longitudinal and lateral turbulence, the vertical turbulence of incident wind also needs to be carefully considered for better wind tunnel simulation of the roof corner pressures, especially for a satisfying simulation of peak suction pressures near the roof corner.

Acknowledgement

The financial support of the US National Science Foundation (Grant No. CMS-9409869) is acknowledged.

References

- Banks, D., Meroney, R.N., Sarkar, P.P., Zhao, Z. and Wu, F. (2000), "Flow visualization of conical vortices on flat roofs with simultaneous surface pressure measurement", *Journal of Wind Engineering and Industrial Aerodynamics*, **84**(1), 65-85.
- Cochran, L.S. and Cermak, J.E. (1992), "Full- and model-scale cladding pressures on the Texas Tech University experimental building", *Journal of Wind Engineering and Industrial Aerodynamics*, **41-44**, 1589-1600.
- CSU/TTU (1998). *CSU/TTU Cooperative Program in Wind Engineering: Progress Report for Technology Assessment and Advisory Council*, Texas Tech University, Lubbock, Texas.
- Ginger, J.D. and Letchford, C.W. (1993), "Characteristics of large pressures in regions of flow separation", *Journal of Wind Engineering and Industrial Aerodynamics*, **49**, 301-310.
- Kawai, H. and Nishimura, G. (1996), "Characteristics of fluctuating suction and conical vortices on a flat roof in

- oblique flow”, *Journal of Wind Engineering and Industrial Aerodynamics*, **60**, 211-225.
- Kawai, H. (1997), “Structure of conical vortices related with suction fluctuation on a flat roof in oblique smooth and turbulent flows”, *Journal of Wind Engineering and Industrial Aerodynamics*, **69-71**, 579-588.
- Letchford, C.W. (1995), “Simultaneous flow visualization and pressure measurements on the Texas Tech building”, *Proceedings of the Ninth International Conference on Wind Engineering*, New Delhi, India.
- Letchford, C.W. and Marwood, R. (1997), “On the influence of v and w component turbulence on roof pressures beneath conical vortices”, *Journal of Wind Engineering and Industrial Aerodynamics*, **69-71**, 567-577.
- Levitan, M.L. and Mehta, K.C. (1992a), “Texas Tech field experiments for wind loads part I: building and pressure measuring system”, *Journal of Wind Engineering and Industrial Aerodynamics*, **41-44**, 1565-1576.
- Levitan, M.L. and Mehta, K.C. (1992b), “Texas Tech field experiments for wind loads part II: meteorological instrumentation and terrain parameters”, *Journal of Wind Engineering and Industrial Aerodynamics*, **41-44**, 1577-1588.
- Lin, J.X., Surry, D. and Tieleman, H.W. (1995), “The distribution of pressure near roof corners of flat roof low buildings”, *Journal of Wind Engineering and Industrial Aerodynamics*, **56**, 235-265.
- Marwood, R. and Wood, C.J. (1997), “Conical vortex movement and its effect on roof pressures”, *Journal of Wind Engineering and Industrial Aerodynamics*, **69-71**, 589-595.
- Mehta, K.C., Levitan, M.L., Iverson, R.E. and McDonald, J.R. (1992), “Roof corner pressures measured in the field on a low building”, *Journal of Wind Engineering and Industrial Aerodynamics*, **41-44**, 181-192.
- Sarkar, P.P., Zhao, Z. and Mehta, K.C. (1997), “Flow visualization and measurement on the roof of the Texas Tech building”, *Journal of Wind Engineering and Industrial Aerodynamics*, **69-71**, 597-606.
- Tieleman, H.W., Surry, D. and Lin, J.X. (1994), “Characteristics of mean and fluctuating pressure coefficients under corner (delta wing) vortices”, *Journal of Wind Engineering and Industrial Aerodynamics*, **52**, 263-275.
- Tieleman, H.W., Surry, D. and Mehta K.C. (1996), “Full/model-scale comparison of surface pressures on the Texas Tech experimental building”, *Journal of Wind Engineering and Industrial Aerodynamics*, **61**, 1-23.
- Tieleman, H.W., Reinhold, T.A. and Hajj, M.R. (1997), “Importance of turbulence for the prediction of surface pressures on low-rise structures”, *Journal of Wind Engineering and Industrial Aerodynamics*, **69-71**, 519-528.
- Wagaman, S.A. (1993). “Full-scale flow visualization over a low-rise building”, Master’s Thesis, Texas Tech University, Lubbock, Texas.
- Wu, F., Sarkar, P.P. and Mehta, K.C. (1999), “Understanding the conical-vortex flow on roofs”, *Proceedings of the Tenth International Conference on Wind Engineering: Wind Engineering into the 21st Century*, Copenhagen, Denmark.
- Wu, F. (2000). “Full-scale study of conical vortices and their effects near roof corners”, Ph.D. Dissertation, Texas Tech University, Lubbock, Texas.
- Zhao, Z. (1997). “Wind flow characteristics and their effects on low-rise buildings”, Ph.D. Dissertation, Texas Tech University, Lubbock, Texas.